

Investigation of Ion-Acoustic-Decay-Instability Thresholds in Laser-Plasma Interactions

K. Mizuno,⁽¹⁾ P. E. Young,⁽³⁾ W. Seka,⁽²⁾ R. Bahr,⁽²⁾ J. S. De Groot,⁽¹⁾ R. P. Drake,⁽¹⁾
and K. G. Estabrook⁽³⁾

⁽¹⁾*Plasma Physics Research Institute, University of California,
and Lawrence Livermore National Laboratory, Livermore, California 94550
and Department of Applied Science, University of California, Davis, California 95616*
⁽²⁾*Laboratory for Laser Energetics, University of Rochester, Rochester, New York 14627*
⁽³⁾*Lawrence Livermore National Laboratory, Livermore, California 94550*

(Received 11 September 1989)

The ion acoustic decay instability has been studied by monitoring the Stokes sideband of the second-harmonic emission from a laser-produced plasma. The intensity threshold decreased as the laser spot size increased. It reached homogeneous-plasma collisional values in planar plasmas produced using large laser spot sizes ($D \gtrsim 600 \mu\text{m}$), for laser wavelengths of either 1.06 or 0.53 μm . These observations show that the ion acoustic decay instability may well play a more important role in laser fusion than had been generally believed.

PACS numbers: 52.40.Nk, 52.35.Mw, 52.50.Jm

The ion acoustic parametric decay instability¹ (IADI), in which an electromagnetic wave decays into an electron plasma wave (EPW) and an ion acoustic wave (IAW) near the critical density N_c (where electromagnetic wave frequency equals plasma frequency), is a fundamentally important subject in plasma physics. In addition, microwave^{2,3} and computer^{4,5} simulations have shown that the EPW product of IADI can produce significant quantities of hot electrons. Such hot electrons are of concern to proposed laser-fusion targets because they can preheat the target and degrade compression. In spite of the simulation results, it had been hoped that IADI would not constrain laser-fusion target designs, for two reasons. First, once the plasma has formed, the laser intensity would be significantly attenuated by collisional absorption before it reached the densities near the critical surface where IADI occurs. Second, the threshold for IADI would be substantially increased by convective stabilization in the steepened density profile near critical density. The present work, however, shows that for conditions now of interest the threshold can be much lower than anticipated. The IADI could be important for laser fusion.

A number of authors⁶⁻¹³ have studied emissions near the second harmonic $2\omega_0$ of the laser frequency from laser-produced plasmas. Emissions at $2\omega_0$ were observed which were attributed^{8,13} to resonance absorption. In addition, a Stokes sideband was often observed that was attributed to the beating^{6,13} of two IADI EPW's, and is thus shifted in frequency from $2\omega_0$ by twice the frequency of the ion acoustic wave driven by the IADI. In the previous experiments, the use of either very short (100 psec) laser pulses, very high laser intensities, or small laser spot sizes produced complicated signals or high threshold values. It had been generally believed that the density profile near N_c would be quite steep even in a high-gain laser-fusion target, due to both ponderomotive

and ablative steepening. As a result, it was anticipated that the threshold of the IADI would be determined by convective losses. Indeed, previous experiments¹³ using relatively small (100 μm) laser spots confirmed these expectations. In contrast to such previous experiments, the present experiments used relatively long laser pulses ($\tau_L \sim 1$ ns) and large ($D \leq 900 \mu\text{m}$) laser spots of relevance to laser fusion. We find that the IADI threshold decreases dramatically and reaches homogeneous-plasma collisional values. These new results indicate that the IADI could potentially impact laser fusion. The experimental observations are discussed next, followed by a suggested explanation, after which the implications for laser fusion are considered.

In the present experiments, the laser intensity (I_L), laser wavelength (λ_0), and laser spot diameter (D) were systematically and independently varied. The experiments were conducted using two laser facilities: the Phoenix (Janus) laser facility at Lawrence Livermore National Laboratory (LLNL) and GDL laser facility at the Laboratory for Laser Energetics (LLE). In all cases, the laser normally irradiated a planar target (CH of 50- μm thickness) with a 1-nsec-FWHM Gaussian pulse and a maximum energy of 200 J. For each laser spot size, the laser intensity was varied by changing the laser energy. We monitored the second-harmonic spectrum by collecting the emission at 135° from the incident laser wave vector and in the plane of the laser electric field. In the experiments at Phoenix, the focusing lens was $f/2$, the signal was collected by an $f/5$ lens, and the time-resolved spectrum was measured using a LLNL streak camera (resolution of 1 \AA and 30 psec). In the experiments at GDL, the focusing lens was $f/3$, and the signal was collected by a focusing mirror. Experiments were conducted using 1.06- μm (at both facilities) and 0.53- μm (at GDL) laser light, and verified the expected

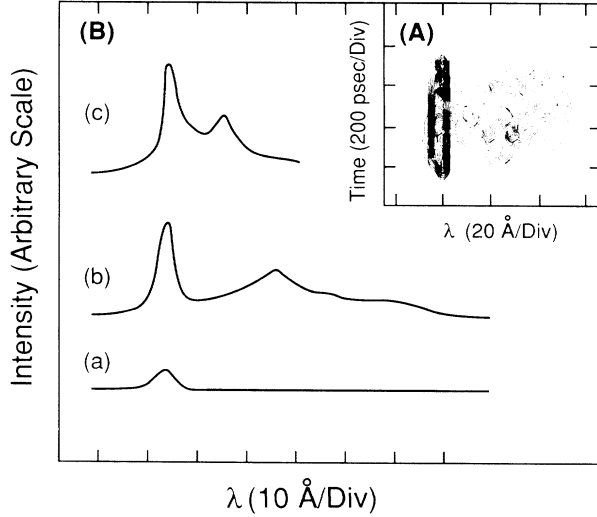


FIG. 1. (a) Two-dimensional contour plot of IADI (the relative intensity vs time and wavelength). $I_L = 6 \times 10^{13}$ W/cm², $\lambda_0 = 1.06$ μ m, and $D = 350$ μ m. (b) Time-integrated spectrum near the second-harmonic frequency for, curve a, $I_L = 5.6 \times 10^{12}$ W/cm², $D = 350$ μ m, $\lambda_0 = 1.06$ μ m; curve b, 3×10^{13} W/cm², $D = 350$ μ m, $\lambda_0 = 1.06$ μ m; and curve c, 3×10^{13} W/cm², $D = 900$ μ m, $\lambda_0 = 0.53$ μ m. The vertical scale for curve c is different from the other curves.

laser-wavelength scaling of the IADI.

Figure 1(a) shows a typical time-resolved spectrum with $I_L = 6 \times 10^{13}$ W/cm². A narrow, strong feature at $2\omega_0$ is clearly observed, and is attributed to resonance absorption as discussed above. The Stokes structure attributed to the IADI is seen to the right (the red side) of the $2\omega_0$ signal, and begins about 100 psec after the onset of the $2\omega_0$ signal. The change in the time-integrated spectrum with laser intensity at a given spot size is illustrated in Fig. 1(b). At a low laser intensity (curve a), emission is observed only at $2\omega_0$. Above a well-defined threshold, the Stokes sideband appears with a wavelength shift $\Delta\lambda \approx 23$ Å (curve b). The intensity of the Stokes sideband was observed to increase strongly with laser intensity near threshold. Curve b also shows a weak second Stokes peak with $\Delta\lambda \approx 46$ Å. No significant anti-Stokes signals were observed. By changing the incident laser wavelength to 0.53 μ m, $\Delta\lambda$ decreases to 12 Å (curve c). This is about half of the value obtained in the experiments with $\lambda_0 = 1.06$ μ m, as expected. As expected, the emissions at $2\omega_0$ were not significantly Doppler shifted.

We found the IADI threshold to be quite sensitive to the laser spot size. The threshold is defined as the laser intensity above which the Stokes mode is observed, and below which no Stokes mode is observed. Figure 2 shows the observed threshold versus laser spot size for 1.06- and 0.53- μ m laser irradiations. For the smallest spot size ($D = 100$ μ m), the threshold is about 6×10^{13} W/cm² for 1.06- μ m laser light, in agreement with the

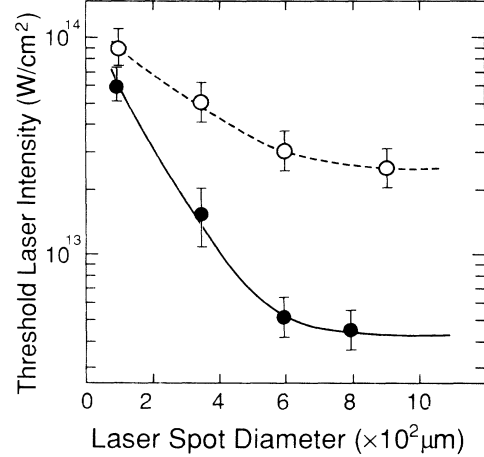


FIG. 2. The threshold vacuum laser intensity for observation of the IADI as a function of the laser spot diameter. Solid circles, 1.06- μ m laser; open circles, 0.53- μ m laser. The 1.06- μ m data are from Phoenix for $D \leq 600$ μ m and from GDL for $D = 800$ μ m.

result of Ref. 13. The threshold value decreases as laser spot size increases, reaching a constant value with a large enough spot size. Similar trends are observed for both 1.06- and 0.53- μ m laser light, with the 0.53- μ m experiments having a higher minimum threshold.

We find the minimum threshold values shown in Fig. 2 to be approximately equal to homogeneous-plasma collisional values. The threshold for the IADI in a homogeneous plasma is¹

$$I_{\theta}^2 = 2.2 \times 10^{16} T_e (\text{keV}) \frac{\Gamma_e}{\omega_0} \frac{\Gamma_i}{k C_s}, \quad (1)$$

in which C_s is the sound speed, Γ_e and Γ_i are the damping rates of the electron plasma waves (collisional and Landau damping) and ion acoustic waves (Landau damping), respectively, and k is the wave number of the ion acoustic wave (which is approximately equal to that of the electron plasma wave). The solid curve a in Fig. 3(a) shows the threshold I_{θ}^2 versus plasma density. As density decreases, the wave number k increases, and once k becomes large enough, Landau damping of the plasma wave rapidly increases, increasing the threshold. The growth rate of the IADI, slightly above threshold, increases approximately as k . Therefore, the location of the observed minimum threshold is near the Landau damping limit at $N_e/N_c \approx 0.86$. The threshold value weakly depends on T_e in the collision-dominated region ($N_e/N_c > 0.86$), being inversely proportional to $\sqrt{T_e}$. In calculating the threshold shown, we used $T_e = 0.4$ keV based on the computer calculations described later. The data point (solid circle) in Fig. 3 shows the observed minimum threshold. The density is determined from the wavelength shift $\Delta\lambda$ using the dispersion relations¹ of the waves involved. The average intensity at the instability

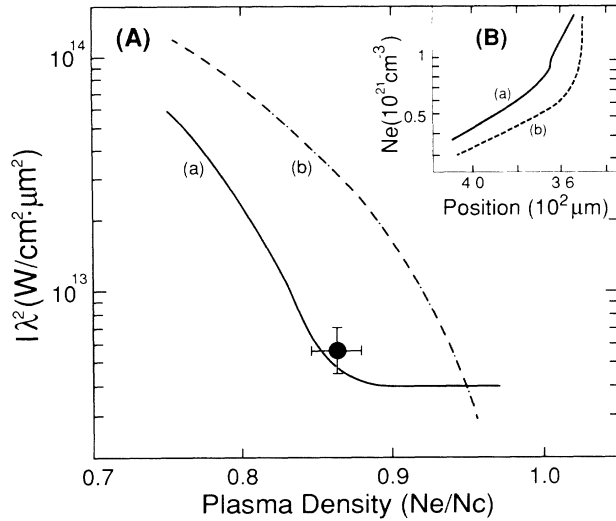


FIG. 3. (A) The observed (solid circle) and calculated (curve *a*) threshold intensity $I\lambda_0^2$ [$(\text{W}/\text{cm}^2)\mu\text{m}^2$] for the IADI in a homogeneous plasma as a function of plasma density, expressed as a fraction of critical density. The calculated density of the underdense plateau is shown vs the local laser intensity by curve *b* ($T_e = 0.4$ keV). (B) Inset: Density-profile calculation for a flux limiter of 0.1 (—) or 0.03 (---).

location was calculated from the incident laser intensity, including effects of collisional absorption and swelling near the critical point. The observed minimum threshold agrees favorably with the calculated minimum. The experiments using $0.53\text{-}\mu\text{m}$ irradiation produced similar results.

The following simple theory gives consistent results with the observed low threshold. Small laser spots (that were smaller than $C_s\tau_L$) produce spherical plasma expansions¹⁴ and, therefore, steep profiles near critical density. This geometric-steepening effect increases the threshold of the IADI. In contrast, for larger spot diameter $D \gg C_s\tau_L$, the plasma expansion can be considered to be planar.¹⁴ In this planar case, one can analytically estimate the underdense plasma density and plasma scale length using a one-dimensional theory.^{5,15} The plasma density is modified by the ponderomotive force^{5,15,16} of the incident laser, and a density profile with a steep density gradient at the critical surface and an underdense plateau is produced. The average plateau density (the horizontal axis) is plotted versus the local laser intensity (the vertical axis) in curve *b* of Fig. 3(A). In the context of early experiments for laser fusion, in which high intensities were reached early in the driver pulse, it had been generally expected that the plasma density profile would be steepened to below the densities at which IADI occurs. Present day design constraints impose more gradual intensity increases with a long duration, implying the importance of the large-spot results of Fig. 3(A). It appears that the threshold curve *a* is well below (or to left-hand side of) curve *b*, showing that the IADI thresh-

old can be reached before the laser intensity becomes large enough for the steepening to become strong. At the threshold laser intensities, the plasma density modification is quite small (as shown in curve *b*) so that the IADI can be excited on the underdense plateau. Computer simulations, discussed next, show that there can be very little ablative steepening, as well.

The hydrodynamic simulations used the LASNEX computer code.¹⁷ Figure 3(B) shows the calculated density profiles for $I_L = 5 \times 10^{12} \text{ W}/\text{cm}^2$ and $\lambda_0 = 1.06 \mu\text{m}$. When the flux limiter¹⁴ was taken to be 0.1, the density-gradient scale length was calculated to be $34 \mu\text{m}$ at $n = 0.86n_c$ (the instability region), which is large enough that the convective threshold¹⁸ becomes comparable to the homogeneous threshold. In contrast, when the flux limiter was taken to be 0.03, the density-gradient scale length was calculated to be only $5 \mu\text{m}$ at $n = 0.86n_c$, which is so small that convective losses should increase the threshold to well above the observed value. Thus, we found that the observed low threshold is consistent with hydrodynamic simulations, but only if the actual density profile corresponds to that calculated using a flux limiter of 0.1, which is well known to be roughly equivalent to classical heat flow in plasmas.

We now consider the implications of the present results for laser fusion. The initial phase of a high-gain, laser-fusion implosion, with a duration of up to several times 10 ns, will employ a low laser intensity to launch an initial, weak shock wave into the fusion fuel. During this period, the target will be particularly sensitive to hot-electron preheat because the Fermi energy of the fuel will still be quite small.¹⁹ Fortunately, the laser intensity will be low enough to avoid most parametric instabilities during this phase. However, the laser light that penetrates to the critical density during at least the first part of this phase may be intense enough to excite the IADI, given the low thresholds discovered in the present work. Whether the IADI will turn out to constrain the design of this phase of the laser fusion implosion, requiring specific tailoring of the laser pulse, the laser wavelength, or the target composition, will depend upon the quantitative examination of several further issues. These include the saturation amplitude of the electron plasma waves, the volume over which they are excited, the efficiency with which they produce hot electrons, and the energy distribution and the transport properties of such electrons. Such issues can be examined by future experiments in relevant plasmas. Already there is evidence, from microwave simulation experiments,^{3,4} that significant electron heating can occur *even when the IADI is weak*, if the unstable volume is large enough. In any event, it is clear that the IADI should be considered in the design of targets for high-gain laser fusion.

We acknowledge the fruitful and stimulating discussions with W. L. Kruer and E. M. Campbell, and the help and encouragement of J. Knaur. This work was supported by the National Laser Users Facility at the

LLE, University of Rochester, with financial support from the U.S. DOE, and was partially supported by the Plasma Physics Research Institute, University of California, Davis, and LLNL, and by Lawrence Livermore National Laboratory under the auspices of the U.S. DOE.

¹K. Nishikawa, J. Phys. Soc. Jpn. **24**, 916 (1968); **24**, 1152 (1968); W. L. Kruer, *The Physics of Laser Plasma Interactions* (Addison-Wesley, Reading, MA, 1988).

²K. Mizuno, J. S. De Groot, and K. G. Estabrook, Phys. Rev. Lett. **52**, 271 (1984); Phys. Fluids **29**, 568 (1986).

³K. Mizuno *et al.*, Phys. Rev. A **38**, 4344 (1988).

⁴P. W. Rambo *et al.*, Phys. Fluids **27**, 2234 (1984).

⁵K. Estabrook and W. L. Kruer, Phys. Fluids **26**, 1888 (1983).

⁶C. Yamanaka *et al.*, Phys. Rev. Lett. **32**, 1038 (1974).

⁷J. L. Bobin *et al.*, Phys. Rev. Lett. **30**, 594 (1973).

⁸K. Eidman and R. Sigel, Phys. Rev. Lett. **34**, 799 (1975).

⁹N. G. Vasov *et al.*, Zh. Eksp. Teor. Fiz. **76**, 2094 (1979) [Sov. Phys. JETP **49**, 1059 (1979)].

¹⁰X. Zhihan *et al.*, J. Appl. Phys. **54**, 4902 (1983).

¹¹Y. Takada *et al.*, Phys. Fluids **31**, 692 (1988).

¹²P. D. Carter, S. M. L. Sim, and T. P. Huges, Opt. Commun. **27**, 423 (1987).

¹³K. Tanaka *et al.*, Phys. Fluids **27**, 2187 (1984).

¹⁴C. E. Max, Lawrence Livermore Report No. UCRL-53107, Rev. 1 (unpublished).

¹⁵K. Lee *et al.*, Phys. Fluids **20**, 51 (1977).

¹⁶H. Takabe and P. Mulser, Phys. Fluids **25**, 2304 (1982).

¹⁷G. B. Zimmerman and W. L. Kruer, Comments Plasma Phys. Controlled Fusion **2**, 51 (1975).

¹⁸F. W. Perkins and J. Flick, Phys. Fluids **14**, 2012 (1971).

¹⁹J. Meyer Ter Vehn, Nucl. Fusion **22**, 561 (1982).